Non-equilibrium solidification of concentrated Fe–Ge alloys

Krishanu Biswas [a], Gandham Phanikumar [b], Dieter M. Herlach [c],
Kamanio Chattopadhyay [a,*]

[a] *Indian Institute of Science, Bangalore 560012, India*
[b] *Indian Institute of Technology, Madras, Chennai 600036, India*
[c] *Institute for Space Simulation, DLR, D-5117, Köln, Germany*

Abstract

The solidification of concentrated alloys containing ordered compounds is less well understood. These alloys often exhibit complex phase change like peritectic reaction during liquid to solid transformation. The Fe-rich part of Fe–Ge binary alloy system consists of several critical points and ordered–disorder transitions and can be used as a model system to study the effect of departure from equilibrium on the solidification microstructure. In order to understand the phase selection and morphological transitions, undercooling and recalescence behaviour; growth rate of the solidifying phases and microstructure need to be explored. In the present paper, we summarise the results obtained in several iron rich alloy compositions (Fe–(14–25) at.% Ge) using techniques of melt quenching, levitation and laser resolidification. These results provide insight to the current theories of dendritic growth and reveals possibility of a new pathway for phase evolution in peritectic alloys at high undercooling involving a massive transformation.
© 2006 Elsevier B.V. All rights reserved.

Keywords: Undercooling; Containerless processing; Rapid solidification; Metastable phases; Laser resolidification

1. Introduction

Rapid solidification processing enables the study of crystal growth under non-equilibrium conditions. The deviation of the chemical equilibrium at the solid–liquid interface and the kinetic undercooling lead to the metastable phase formation [1]. These thermodynamic and kinetic factors are related to a fundamental parameter, known as melt undercooling. From the point of view of thermodynamics, undercooling of melt is a necessary precondition for metastable phase formation [2]. When the temperature of the melt falls below the virtual melting point of a metastable phase, a finite driving force for nucleation of that phase exists. Nucleation kinetics in the undercooled melt selects the crystallographic phases—stable or metastable.

Nucleation is the process, which initiates the solidification. It is continued by subsequent growth. The conditions underlying the undercooled melt of metals and alloys often lead to the dendritic growth [3]. Heat and mass transports at the solid–liquid interface during dendritic growth determine the conditions for propagation of the solidification front. Growth takes place by attaching more and more atoms at the solid–liquid interface. The velocity of the solid–liquid interface depends on the interface conditions [4] and is given by:

$$V = V_0 \left[1 - \exp\left(-\frac{\Delta G}{RT_i} \right) \right], \tag{1}$$

where V is the solid–liquid interface velocity, T_i the interface temperature, ΔG the free energy change for crystallization at a given undercooling ΔT and R is the universal gas constant. The V_0 is the kinetic parameter. V_0 depends on the atomic attachment kinetics. It can be scaled with the interface diffusive speed (V_D) for diffusion-limited or speed of sound (V_s) for collision-limited growth. The role of attachment kinetics on the dendrite growth becomes important as the velocity of the solid–liquid interface increases.

In the present paper, we review our investigations on nucleation and phase selection during solidification of concentrated iron rich Fe–Ge alloys away from the equilibrium conditions. We will present three separate cases where nucleation kinetics and issues in phase selection [5–7] will be discussed. These results are produced using samples processed by three different

non-equilibrium techniques, namely melt spinning, levitation and laser resolidification. The alloy compositions studied are Fe–14.2 at.% Ge, Fe–18 at.% Ge and Fe–25 at.% Ge [8]. The solidification of Fe–14.2 at.% Ge and Fe–18 at.% Ge starts with nucleation of bcc α-FeGe ($a = 0.288$ nm) solid solution. In case of Fe–18 at.% Ge alloy, under non-equilibrium conditions, α_2 (B2) phase can have finite driving force for nucleation when the liquid is undercooled more than 100 K. Therefore, there exists a possibility of nucleating metastable α_2 as compared to stable α phase at this composition. The α_2 phase again orders in solid state to form α_1 (DO$_3$, $a = 0.576$ nm) phase. The situation is different in case of Fe–25 at.% Ge alloy. On cooling a liquid of Fe–25 at.% Ge composition, the first phase that forms from the liquid is α_2. This phase upon further cooling transforms to ε (DO$_{19}$, $a = 0.5169$ nm, $c = 0.4222$ nm) by a peritectic reaction with the remaining liquid at 1122 °C. However, the peritectic reaction being diffusion controlled, usually does not proceed to completion and hence leads to a phase mixture in the final microstructure [9]. Attention is also drawn to the eutectic reaction L → ε + β close to the composition chosen for this study, where β phase has hexagonal structure (B8$_2$, $a = 0.3998$ nm and $c = 0.501$ nm). One can clearly see that rapid solidification using the undercooling technique provides a possibility to suppress the peritectic reaction and solute partitioning to obtain a phase pure ε [7]. Further, the sluggish nature of the transformation ε → ε′ (L1$_2$, $a = 0.3665$ nm) [10] can enable the metastable ε to be retained at the room temperature.

2. Experimental

The rapid solidification experiments are carried out at Indian Institute of Science, Bangalore, by twin roller quenching as well as melt spinning technique using a copper wheel. The undercooling experiments are carried out at DLR, Köln, Germany using electromagnetic levitation facility. Growth rate of the solid–liquid interface was measured using the capacity proximity sensor method. Complete details of the growth rate measurement setup are available elsewhere [11,12]. The laser resolidification experiments were carried out using a 10 kW CO$_2$ laser at University of Clausthal, Germany.

3. Results and discussion

In the case of Fe–14.2 at.% Ge alloy, the basic idea has been to explore the possibility of congruent ordering and to study the effect of conditional spinoidal on the microstructural evolution [5]. The phase diagram [8] indicates that rapidly solidified alloy will pass through the α_2 to ($\alpha_2 + \alpha_1$) phase field. Therefore, there is always a possibility of solid state ordering of the twin-roller quenched sample. The selected area diffraction (inset of Fig. 1) pattern indicates presence of DO$_3$ ordering. Fig. 1 shows the dark field image revealing the presence of relatively distinct B2 domains in the rapidly solidified state. The domain boundaries are isotropic in nature. We also note the contrast inside the domains, suggesting additional boundaries inside the coarser domains. The morphology of the domains suggests transformation of disorder α into an ordered B2 structure at higher
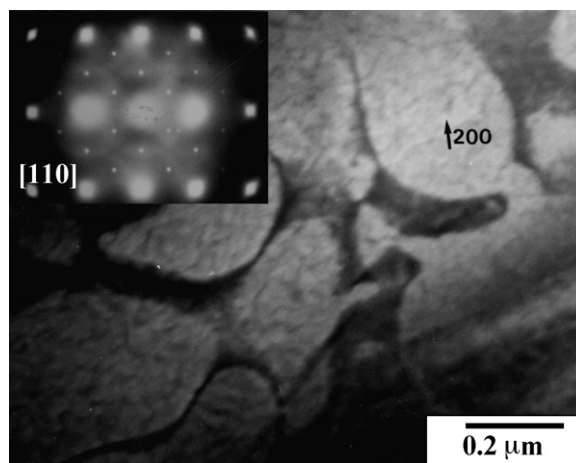

Fig. 1. Dark-field image of Fe–14.2 at.% Ge alloy taken using the 2 0 0 reflection showing up distinct B2 domains. The selected-area diffraction pattern along [1 1 0] is shown as inset.

temperature. The presence of tricritical point in the phase diagram indicates that the transformation to low temperature DO$_3$ phase can take a complicated route. The B2 phase can transform to the DO$_3$ phase through a continuous transformation if nucleation can be suppressed at the bimodal boundary due to rapid cooling rate. In that case, the system can change to the DO$_3$ ordered stage by a second order transformation. This will be followed by a conditional spinoidal and renucleation of the B2 phase in the Ge lean regions. Systematic dark field imaging using unique DO$_3$ reflection (for details see [5]) in addition to the B2 reflection indicates the presence of finer DO$_3$ domains within the coarse B2 domains. The finer contrast inside the large B2 domains suggests the presence of B2 boundary due to renucleation at a later stage. Together, these evidences suggest that rapid quenching technique can lead to formation of disorder α solid solution, which transforms to B2 ordered grains followed by second order DO$_3$ ordering. This leads to a conditional spinoidal followed by a renucleation of ordered B2 at the Fe rich regions to achieve the final microstructure.

As the germanium concentration in the alloy increases, the B2 phase field expands gradually to solidus temperature. Therefore, the phase competition between the B2 and disordered bcc phase during rapid solidification is expected to come into play for higher germanium concentrations. Fe–18 at.% Ge composition in the phase diagram lies on the edge of bcc to B2 order–disorder transitions at the solidus. In order to understand the nucleation and growth kinetics during solidification quantitatively, we have utilized the electro-magnetic levitation facility at DLR. Dendrite growth velocities of Fe–18 at.% Ge alloy were measured as a function of undercooling. A summary of the velocity–undercooling relationship obtained from a large number of experiments is shown in Fig. 2. The undercooling is given by the difference between the liquidus temperature and nucleation temperature of the alloy.

The experimental data on the dendrite growth measurements has been analyzed within the frame work of dendrite growth model by Boettinger, Corriell and Trivedi (BCT model) [13], modifying the work of Lipton, Kurz and Trivedi (LKT model)
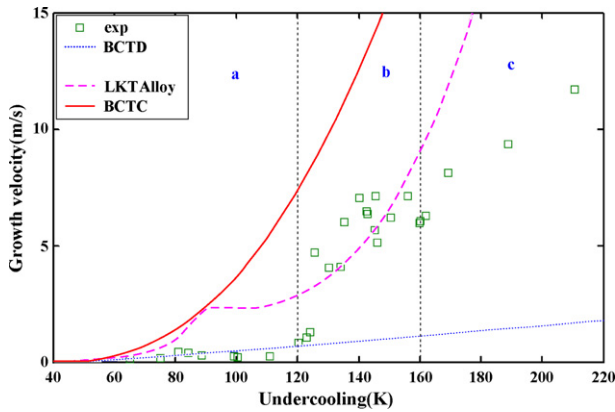
Fig. 2. Measured and computed growth rate curves for Fe–18 at.% Ge alloy.

[14]. The model calculations involve a velocity dependence of partition coefficient and liquidus slope. We refer to textbooks for basic equations [15].

Theoretical and experimental results are plotted in Fig. 2. One can find that none of the theoretical plots falls on the experimental data points throughout the whole undercooling range studied. The experimental measurements can be divided into three growth regimes as shown in Fig. 2:

(a) Low-undercooling regime ($\Delta T < 120$ K), where the data points can be fitted with BCT model using a low kinetic coefficient (μ) corresponding to $V_0 = V_D$.
(b) Intermediate-undercooling regime, which starts with a jump in the growth velocity at about 120 K undercooling. The experimental results could be fitted using collision limited growth model (LKT) using μ corresponding to $V_0 = V_s$.
(c) High-undercooling (>160 K) regime where the BCT and LKT model overestimate the growth rate. No agreement with other available dendritic growth theories could be found.

This theoretical analysis can be substantiated by transmission electron microscopy (TEM) examination of the undercooled samples. The dark field image taken using B2 superlattice reflection of (2 0 0) type (Fig. 3) shows the presence of coarse and isotropic B2 domains. The [0 1 1] pattern (as shown as inset 1 of Fig. 3) clearly indicates the presence of DO$_3$ ordering in the sample. The dark-field image (inset 2 of Fig. 3) using (1 1 $\bar{1}$) reflections lights up very fine-scale DO$_3$ domains inside the B2 domains. Presence of a large number of anti-phase domains suggests that the bcc phase has nucleated directly from the liquid and has undergone ordering reaction in solid state. TEM analyses of samples undercooled below 110 K (not shown here) do not show B2 domains. Therefore, growth kinetics plays a very important role in phase selection for this alloy composition.

In the case of Fe–25 at.% Ge alloy, the solidification behaviour is quite complex. The temperature–time profiles of this alloy indicate the presence of two nucleation events both at high and low levels of undercoolings. The first one corresponds to the formation of α_2 and second one is for ε phase formation via a peritectic reaction involving α_2 and liquid. The time
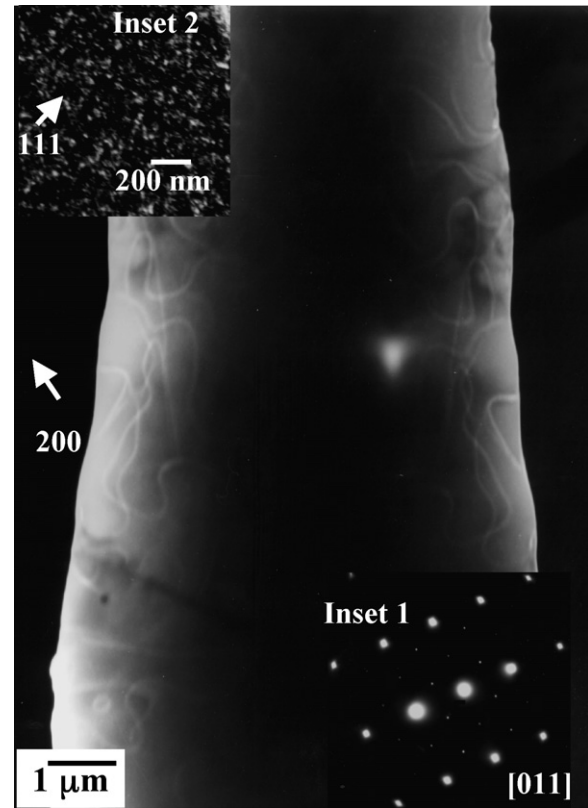

Fig. 3. Dark-field image obtained using the 2 0 0 reflection from Fe–18 at.% Ge sample undercooled by 140 K lighting up B2 domains with inset 1 showing [0 1 $\bar{1}$] zone-axis pattern and inset 2 showing the presence of fine-scale DO$_3$ domains.

difference between the appearances of two nucleation events is found to vary from 0.5 to 4 s depending on the levels of undercooling. In the following sections, we will first summarise the microstructural evidences obtained by us followed by an analysis on growth kinetics to understand the growth behaviour of the ordered intermetallic phases.

Fig. 4a and b show microstructures of samples solidified at different undercoolings. For sample undercooled by 120 K, the solidified microstructure (Fig. 4a) reveals presence of primary α_2, peritectic ε phase and interdendritic ε–β eutectic. The presence of all the three phases has been confirmed by TEM analysis [7]. This kind of morphology of the phases is typical of a peritectic reaction [9]. The peritectic reaction, L + $\alpha_2 \rightarrow \varepsilon$ indicates that the ε phase must nucleate at the α_2 (dendrite)–L interface and propagate to consume the α_2 phase. This kind of morphology is often termed as 'cap morphology' as the peritectic phase ε forms a cap over the primary phase α_2. An important feature of the microstructure is the concavity of the residual α_2–ε interface towards the centre of the α_2 dendrite. The presence of $\varepsilon + \beta$ eutectic in the microstructure in all the samples indicates that inter-dendritic liquid has solidified through a L $\rightarrow$ $\varepsilon + \beta$ eutectic reaction.

For samples solidified at higher levels of undercooling, the microstructure consists predominantly of ε-phase. In fact, cap morphology, which is a signature of peritectic reaction, could not be observed in any of the samples with undercooling larger than
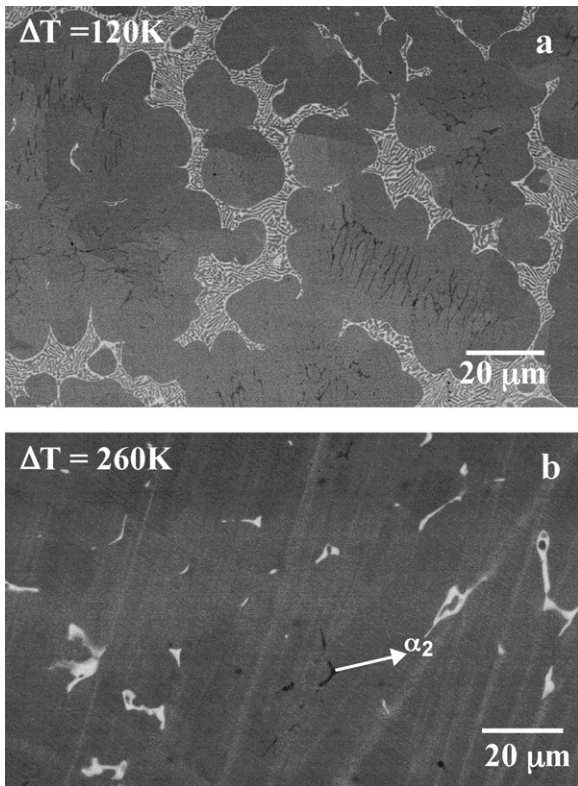
Fig. 4. Back scattered-electron micrographs of Fe–25 at.% Ge alloy solidified at different levels of undercooling: (a) 120 K and (b) 260 K.

120 K. In these samples, one can find traces of β phase outlining the original dendritic microstructure. Samples solidified at undercoolings near and above 165 K (not shown here) contained ε-phase with ε–β eutectic. No trace of α_2 could be observed in

this sample. Both lamellar and rod like morphology of eutectic has been observed for highly undercooled samples [7]. Fig. 4b shows the SEM micrograph of a sample undercooled by 260 K prior to first nucleation event. One can find that the microstructure consists of predominantly ε with miniscule amount of α_2 (shown by white arrow on the figure). The presence of β as white network delineating the dendrite structure can also be found.

TEM studies of highly undercooled samples give insight to the nature of the phase selection. Fig. 5 shows bright field image of a sample undercooled to 165 K showing residual α_2 in contact with ε phase. The ε phase is found to be growing from the surface of α_2. The SAD pattern obtained from both the α_2 and ε phases are shown as insets on the Fig. 5. The ordered nature of both phases is clear. The α_2–ε interface is not clean. One can observe the dislocation debris at the growing ε–α_2 interface. Dark field image using superlattice reflections of ε phase lights up fine scale ordered domains. Dark field image of α_2 phase taken using superlattice reflections of B2 phase reveals that there are no anti-phase domains within α_2 phase. This indicates that α_2 solidified primarily as an ordered (B2) phase. Similar observations have also been made in case of sample undercooled by 260 K. The compositional measurements of the residual α_2 (24.5 at.% Ge) and ε (25 at.% Ge) indicate that both the phases have almost same composition in the highly undercooled samples (165 and 260 K).

Fig. 6 summarises the growth velocity of the primary phase α_2 as a function of levels of undercooling. The growth rate of α_2 phase is found to be sluggish (~0.25 m/s) up to an undercooling level of about 110 K. The growth velocity increases steadily to reach 1.5 m/s at an undercooling of 200 K. The measured solidification time varies from 4 to 25 ms. This is nearly two orders of magnitude smaller than the time delay between the
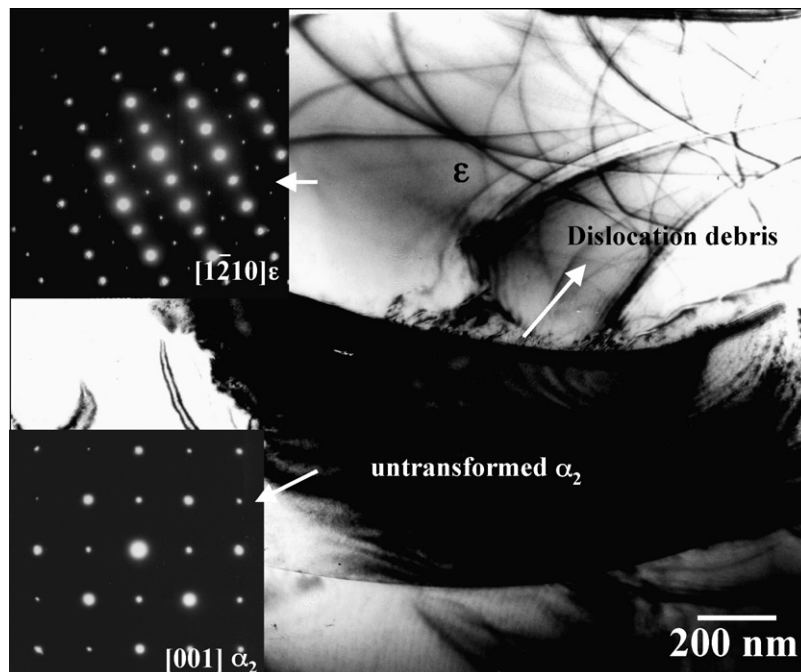

Fig. 5. (a) Bright-field image of Fe–25 at.% Ge alloy undercooled by 165 K showing the growth of ε from primary α_2 phase. The insets show the selected-area diffraction patterns from ε and α_2 phases indicating the ordered nature of phases.
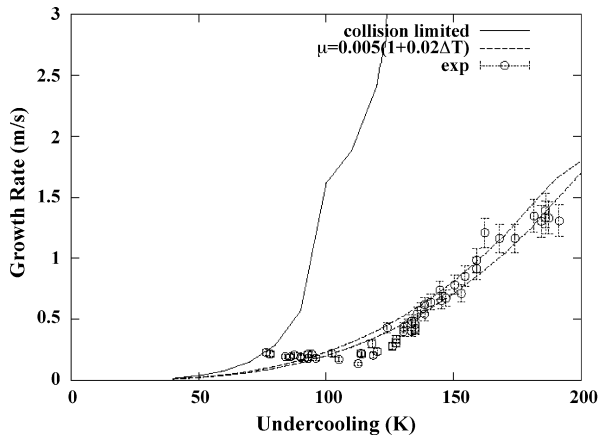
Fig. 6. Measured and computed growth rate curves for Fe–25 at.% Ge alloy [7].

two recalescence events corresponding to nucleation of α_2 and ε as mentioned earlier. Therefore, the measured growth velocity corresponds completely to the primary phase α_2. The error bars in the Fig. 6 indicates the error in the measurement of growth rate. The error is estimated to be a maximum of 10% at all the undercooling. The measured dendrite growth velocity has been analysed within the framework of the BCT theory [13]. Fig. 6 shows that the assumption of collision limited growth leads to overestimation of growth rates. This is understandable as we are dealing with growth of an ordered (B2) phase. According to the disorder trapping model proposed by Aziz and Boettinger [16,17], the kinetic factor controlling the growth of ordered phases is the interface diffusive speed, V_D which has a value three order of magnitude lower than V_s. Several studies [18–20] have indicated that a reduced value of the kinetic coefficient μ is able to fit the computed growth rate of ordered phase in undercooled melt to the experimental data closely. This kind of analysis is shown in the Fig. 6. The composition of the undercooled droplets is found to be Fe–24.5 at.% Ge as measured by electron microprobe analyzer. However, the experimentally observed growth rate cannot be fitted using this composition of the alloy. Therefore, we have tried to fit the experimental data points using compositions lying within a bound of 22 and 25 at.% Ge. The two dashed curves shown in figure for Fe–22 at.% Ge and Fe–25 at.% Ge lay close to each other and envelope the experimental data within the estimated error limits. Another important aspect of the growth of the α_2 phase is that no single value of μ is able to describe the complete experimental data set satisfactorily. As the proper thermodynamic data in this system is not available in the literature, we have taken the μ to be a simple linear function of undercooling for this purpose. Using $\mu = 0.005[1 + 0.02\Delta T]$, the experimental data points can be fitted with computed growth curve. The function used corresponds to the effective value of V_D ranging from 5 to 15 m/s.

The microstructural analysis indicates that as the level of undercooling increases, the microstructure consists of predominantly ε phase with minute traces of α_2. The data from synchrotron experiments [7] indicate the nucleation of α_2 phase followed by ε phase, suggesting typical peritectic reaction taking place during the process of the solidification. Even at higher

levels of undercooling (193 K), evidence indicates the first phase to be nucleated from the undercooled melt is α_2. Therefore, it is clear that both at low and high levels of undercooling, it is the primary phase (α_2), which nucleates first from the undercooled melt.

The microstructure of samples solidified at undercooling larger than 120 K show nearly phase-pure ε. The negligible amount of residual α_2 phase and progressive disappearance of inter-dendritic eutectic phases in these samples indicate completion of peritectic reaction. The dendrite growth analysis in the undercooled melt shows that the secondary arms develop much later than the primary trunk. As the peritectic reaction is diffusion controlled, the length scale of the secondary arm (λ_f) will give an idea about the completion of the peritectic reaction. The simplified expression of λ_f due to Kirkwood [21] is shown to provide a reasonable estimate of λ_f during solidification. The value of the secondary spacing critically depends on the time of solidification, t_f [22]. This time t_f in the present case can be obtained from the time-resolved synchrotron spectra and corresponds to the interval between the appearance of α_2 peak and ε peak in the spectra. This value is found to be close to 10 s. Using this value of t_f and proper values of the other parameters [7], the estimated secondary arms spacing is found to be 23 μm. This value is close to the observed values from the microstructures. Using the diffusivity of Ge in bcc Fe at 1435 as 7.033×10^{-13} m²/s [23], and the maximum time duration between first appearance of ε phase till complete disappearance of α_2 phase to be about 10 s [7], gives us a diffusion distance of 2.6 μm. Therefore, the diffusion distance in solute is found to be much smaller than secondary arm spacing. This clearly indicates that the peritectic reaction (which is limited by solute diffusion in solid phase) is not likely to go to completion.

Therefore, we need to explore other possibilities of formation of phase pure ε. One of them is that the ε phase can form by a solid state transformation from α_2. The TEM micrograph as shown in Fig. 5 suggests the same. The presence of large number of antiphase domains inside ε phase indicates that the ordering has taken place in the solid state. On the other hand, lack of domains inside the α_2 phase suggests that it has been nucleated as ordered B2 directly from the undercooled liquid. The composition analysis of the ε and α_2 phases in the deeply undercooled samples shows that the compositions of these two phases are similar. The solid state transformation requires there is little or no change in composition needed if such a transformation were to take place. The presence of dislocation debris at the α_2–ε interface (Fig. 6) confirms the fact that ε phase has formed by a solid state transformation from α_2 phase. Massive Transformations of bcc → hcp are well known in literature [24]. Thus we suggest that at high undercooling, peritectic reaction is suppressed and ε phase forms via a solid state transformation.

On the other hand, the formation of ε phase can be completely suppressed in a situation when the phase selection occurs by growth competition. The laser resolidification experiment is ideal to study such a growth competition. Fig. 7 shows a scanning electron microscopy (SEM) image of the remelted pool when the laser scanning speed (V_b) used is 0.05 m/s. The inset shows the higher-magnification SEM images The TEM inves-
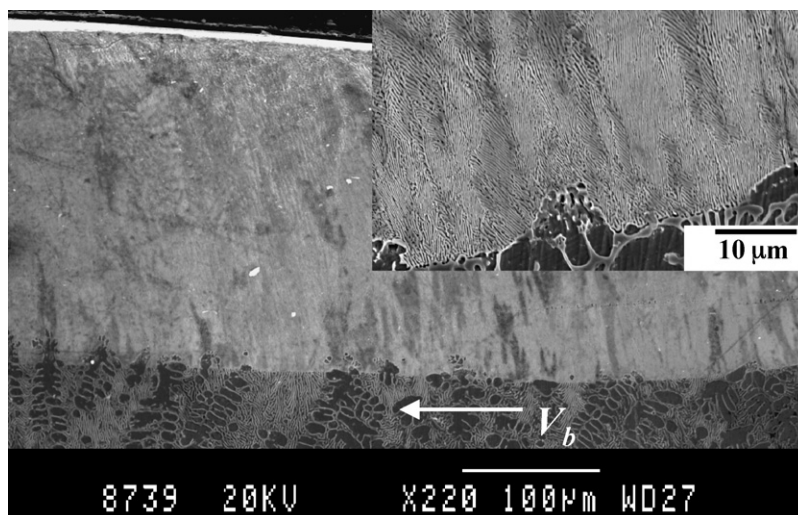
Fig. 7. Low-magnification SEM image of laser-resolidified Fe–25 at.% Ge alloy with (inset) higher-magnification micrograph showing the presence of α_2–β eutectic.

tigation indicates that this is a metastable eutectic between α_2 and β [25]. Thus the microstructural evolution indicates that the growth competition governs the formation of a metastable eutectic α_2–β, as opposed to the stable eutectic, ε–β.

4. Conclusion

It is shown that the understanding the solidification behaviour away from the equilibrium for the concentrated alloys containing ordered phases provide challenge to rapid solidification community. The pathways can differ depending on whether the solidification is nucleation controlled or growth controlled. One, therefore, needs to carry out different sets of rapid solidification experiments. In the example presented here, Fe–Ge alloys can solidify through a new pathway of massive transformation at high undercooling in levitation experiments while laser resolidification yields suppression of the ordered peritectic phase leading to a metastable eutectic growth. Generally the growth rate measurements can be successfully rationalised with existing growth theories while at very high undercooling, our knowledge is less adequate.

References

[1] D.M. Herlach, Mater. Sci. Eng. Rep. R12 (1994) 177.
[2] D. Turnbull, Metall. Trans. A 12 (1981) 695.
[3] J.S. Langer, Rev. Mod. Phys. 52 (1980) 1.
[4] D. Turnbull, J. Chem. Phys. 62 (1962) 609.
[5] K. Raviprasad, S. Ranganathan, K. Chattopadhyay, Scripta Metall. Mater. 26 (1992) 467.
[6] K. Biswas, G. Phanikumar, K. Chattopadhyay, T. Volkmann, O. Funke, D. Holland-Moritz, D.M. Herlach, Mater. Sci. Eng. A 375–377 (2004) 80.
[7] G. Phanikumar, K. Biswas, O. Funke, D. Holland-Moritz, D.M. Herlach, K. Chattopadhyay, Acta Mater. 53 (2005) 3591.
[8] T.B. Massalski, Binary Alloy Phase Diagrams, 2nd ed., ASM, Metal Park, Ohio, USA, 1990, p. 1704.
[9] H.W. Kerr, W. Kurz, Int. Mater. Rev. 41 (1996) 129.
[10] A.H.W. Ngan, I.P. Jones, R.E. Smallman, Mater. Sci. Eng. A 153 (1992) 387.
[11] E. Schleip, R. Willnecker, D.M. Herlach, G.P. Görler, Mater. Sci. Eng. A 98 (1988) 39.
[12] K. Eckler, M. Kratz, I. Egry, Rev. Sci. Instrum. 64 (1993) 2639.
[13] W.J. Boettinger, S.R. Corriell, R. Trivedi, in: R. Mehrabian, P.A. Parrish (Eds.), Proceedings of the Fourth Conference on Rapid Solidification Processing: Principles and Technologies, Baton Rouge (LA), Claitors City, 1987, p. 13.
[14] J. Lipton, W. Kurz, R. Trivedi, Acta Metall. 35 (1987) 957.
[15] W. Kurz, D.J. Fisher, Fundamentals of Solidification, Trans Tech Publication, Aedermannsdorf, 1992, p. 133ff.
[16] W.J. Boettinger, M.J. Aziz, Acta Metall. Mater. 37 (1989) 3379.
[17] M.J. Aziz, W.J. Boettinger, Acta Metall. Mater. 42 (1994) 527.
[18] M. Barth, B. Wei, D.M. Herlach, B. Feuerbacher, Mater. Sci. Eng. A 178 (1994) 305.
[19] K. Eckler, F. Gärtner, H. Assadi, A.F. Norman, A.L. Greer, D.M. Herlach, Mater. Sci. Eng. A 226–228 (1997) 410.
[20] R. Goetzinger, M. Barth, D.M. Herlach, O. Hunziker, W. Kurz, Mater. Sci. Eng. A 226–228 (1997) 415.
[21] D.H. Kirkwood, Mater. Sci. Eng. 73 (1985) L1.
[22] M. Chen, T.Z. Kattamis, Mater. Sci. Eng. A 247 (1998) 239.
[23] E.A. Brandes, Smithells Metals Reference Book, 6th ed., Butterworth & Co Publications Ltd., London, 1983.
[24] R.N. Shiegeto, K. Hirostsi, A. Masato, Mater. Sci. Eng. A 312 (2001) 77.
[25] K. Biswas, K. Chattopadhyay, Metal. Mater. Trans A. (2006) in press.